ORGANIC LETTERS

2011
Vol. 13, No. 18
4962–4965

New A-A-D-A-A-Type Electron Donors for Small Molecule Organic Solar Cells

Li-Yen Lin,[†] Chih-Wei Lu,[‡] Wei-Ching Huang,[‡] Yi-Hong Chen,[‡] Hao-Wu Lin,*[,‡] and Ken-Tsung Wong*[,†]

Department of Chemistry, National Taiwan University, Taipei 10617, Taiwan, and Department of Materials Science and Engineering, National Tsing Hua University, Hsin Chu 30013, Taiwan

hwlin@mx.nthu.edu.tw; kenwong@ntu.edu.tw

Received August 3, 2011

ABSTRACT

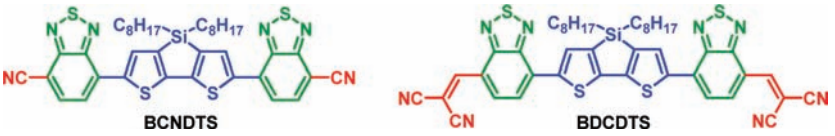

Two A-A-D-A-A-type molecules (BCNDTS and BDCDTS), where two terminal electron-withdrawing cyano or dicyanovinylene moieties are connected to a central dithienosilole core through another electron-accepting 2,1,3-benzothiadiazole block, have been synthesized, characterized, and employed as electron donors for small molecule organic solar cells. Vacuum-deposited bilayer and planar mixed heterojunction devices based on BCNDTS and fullerene acceptors (C_{60} or C_{70}) exhibited decent power conversion efficiencies of 2.3% and 3.7%, respectively.

Organic photovoltaics (OPVs) are emerging as a clean and competitive renewable energy resource due to their unique features including low-cost manufacturing, light weight, and mechanical flexibility.[1] Intensive interdisciplinary efforts have been dedicated to improving the power conversion efficiencies (PCEs) of solution-processed polymer bulk heterojunction (BHJ) solar cells.[2] Organic solar cells employing small molecules as electron donors have also received great attention.[3] To date, small molecule organic solar cells (SMOSCs) based on p-type small molecules and n-type fullerene derivatives have been realized with PCEs in excess of 5% by using either solution-processed[4] or vacuum-deposited[5] fabrication techniques. Moreover, a PCE of up to 8.3% efficiency has been achieved with a vacuum-deposited tandem cell.[6]

Regarding the recent developments of solar-absorbing materials utilized in SMOSCs, the intrinsic properties of commercially available fullerenes such as high electron affinities and superior electron mobilities make them the best acceptor components in contemporary OPV devices.[2a] Thus, the search for new donor materials with appropriate physical properties such as low bandgaps, suitable energy levels, high crystallinity, decent solubility, etc. has taken center stage. Along this line, a large number of donor molecules have been extensively investigated with varying degrees of success. Among them, the symmetrical acceptor–donor–acceptor (A-D-A) or donor–acceptor–donor (D-A-D) systems represent the most ubiquitous molecular architectures, where a wide variety of electron-withdrawing groups, such as squaraine,[4] dicyanovinylene,[5]

(1) (a) Tang, C. W. *Appl. Phys. Lett.* **1986**, *48*, 183. (b) Krebs, F. C. *Sol. Energy Mater. Sol. Cells* **2009**, *93*, 394.

(2) (a) Cheng, Y. J.; Yang, S. H.; Hsu, C. S. *Chem. Rev.* **2009**, *109*, 5868. (b) Wong, W. Y.; Ho, C. L. *Acc. Chem. Res.* **2010**, *43*, 1246. (c) Liang, Y. Y.; Xu, Z.; Xia, J. B.; Tsai, S.-T.; Wu, Y.; Li, G.; Ray, C.; Yu, L. P. *Adv. Mater.* **2010**, *22*, E135.

(3) (a) Lloyd, M. T.; Anthony, J. E.; Malliaras, G. G. *Mater. Today.* **2007**, *10*, 34. (b) Roncali, J. *Acc. Chem. Res.* **2009**, *42*, 1719. (c) Walker, B.; Kim, C.; Nguyen, T. Q. *Chem. Mater.* **2011**, *23*, 470. (d) Cravino, A.; Leriche, P.; Alévêque, O.; Roquet, S.; Roncali, J. *Adv. Mater.* **2006**, *18*, 3033. (e) Kronenberg, N. M.; Steinmann, V.; Bürckstümmer, H.; Hwang, J.; Hertel, D.; Würthner, F.; Meerholz, K. *Adv. Mater.* **2010**, *22*, 4193. (f) Shang, H. X.; Fan, H. J.; Liu, Y.; Hu, W. P.; Li, Y. F.; Zhan, X. W. *Adv. Mater.* **2011**, *23*, 1554. (g) Steinberger, S.; Mishra, A.; Reinold, E.; Müller, C. M.; Uhrich, C.; Pfeiffer, M.; Bäuerle, P. *Org. Lett.* **2011**, *13*, 90.

(4) Wei, G. D.; Wang, S. Y.; Sun, K.; Thompson, M. E.; Forrest, S. R. *Adv. Energy Mater.* **2011**, *1*, 184.

(5) Fitzner, R.; Reinold, E.; Mishra, A.; Mena-Osteritz, E.; Ziehlke, H.; Körner, C.; Leo, K.; Riede, M.; Weil, M.; Tsaryova, O.; Weiß, A.; Uhrich, C.; Pfeiffer, M.; Bäuerle, P. *Adv. Func. Mater.* **2011**, *21*, 897.

(6) Service, R. F. *Science* **2011**, *332*, 293.

(7) Liu, Y.; Wan, X.; Wang, F.; Zhou, J.; Long, G.; Tian, J.; You, J.; Yang, Y.; Chen, Y. *Adv. Energy Mater.* 2011, Epub ahead of print, DOI: 10.1002/aenm.201100230.

10.1021/ol2021077
Published on Web 08/23/2011

alkyl cyanoacetate,[7] 2,1,3-benzothiadiazole,[8] thiadiazolo-[3,4-c]pyridine,[9] diketopyrrolopyrrole,[10] isoindigo,[11] tetracyanobutadiene,[12] and borondipyrromethene,[13] are combined with electron-donating oligothiophenes and/or arylamines. Through a judicious combination of donors and acceptors, the energy levels and bandgaps of these quadrupolar chromophores can be readily modulated. However, there are only a few examples exhibiting remarkable success with this molecular design, rendering the development of new molecular architectures to pursue the so-called "ideal donor molecules" a main focus of SMOSCs research.

In this letter, we report the synthesis, characterization, and photovoltaic application of two A-A-D-A-A-type small molecules (**BCNDTS** and **BDCDTS**, Scheme 1), in which two terminal electron-withdrawing cyano or dicyanovinylene moieties are connected to a central dithienosilole (DTS) core through another electron-accepting 2,1,3-benzothiadiazole (BT) block. The central dithienosilole unit adopted here is a versatile p-type building block for the development of various optoelectronic materials.[14] Specifically, BHJ solar cells based on DTS-containing conjugated polymers have exhibited respectable PCEs of up to 7.3%,[15] benefiting from their better packing abilities and higher hole mobilities as compared to those of the carbon-based homologues.[16] We envisioned that the A-A-D-A-A molecular configuration would not only possess deep-lying highest occupied molecular orbital (HOMO) energy levels but also exhibit better light-harvesting abilities in comparison to the A-D-A counterparts due to the extension of conjugated π-systems and the fortified quinoidal character of conjugated backbones.

Scheme 1. Synthesis of **BCNDTS** and **BDCDTS**

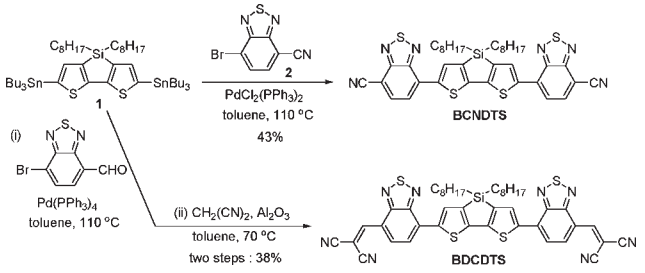

The synthetic routes to the target compounds **BCNDTS** and **BDCDTS** are depicted in Scheme 1, and the synthesis of the building blocks **1** and **2** is shown in Scheme S1 in Supporting Information. Stille coupling reaction of the distannyl derivative **1** with **2** afforded **BCNDTS** in 43% yield. **BDCDTS** was obtained with a yield of 38% via a two-step process where the first involved a Stille coupling reaction of the distannyl derivative **1** with 7-bromo-2,1,3-benzothiadiazole-4-carbaldehyde, subsequently followed by Knoevenagel condensation with malononitrile.

The thermal stability of **BCNDTS** and **BDCDTS** was investigated by thermogravimetric analysis (TGA), which showed the decomposition temperature (T_d) (5% weight loss) to be 378 and 312 °C for **BCNDTS** and **BDCDTS**, respectively (Figure S1 in Supporting Information). The inferior thermal stability for **BDCDTS** is attributed to the presence of the fragile dicyanovinylene moieties.

The electrochemical properties of **BCNDTS** and **BDCDTS** were probed by cyclic voltammetry (CV). As shown in Figure 1, both compounds exhibited one quasi-reversible oxidation wave, corresponding to the oxidation of the central DTS donor. In the cathodic potential regime, four quasi-reversible reduction waves were observed for **BCNDTS**. The first two waves can be attributed to the stepwise reduction of the cyano groups, whereas the third wave can be assigned to the reduction of the BT fragments. On the other hand, **BDCDTS** showed three quasi-reversible reduction waves, and the first and second wave can be ascribed to the reduction of the dicyanovinylene and BT blocks, respectively. Moreover, it is worthy to note that all the reduction potentials of **BDCDTS** are more positive than those of **BCNDTS** (Table 1), reflecting the stronger electron-withdrawing nature of the dicyanovinylene acceptors.

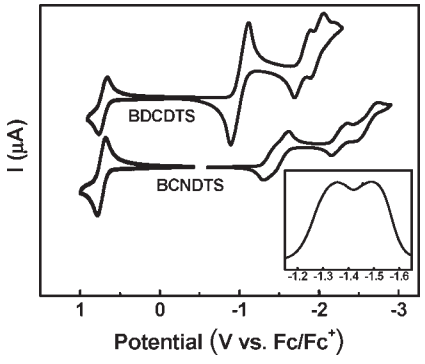

Figure 1. Cyclic voltammograms of **BCNDTS** and **BDCDTS**. All potentials were recorded versus ferrocene/ferrocenium (Fc/Fc^+) as an external reference. Inset: the selected reduction region of the differential pulse voltammogram of **BCNDTS**. Scan rate: 100 mV/s.

(8) (a) Li, W.; Du, C.; Li, F.; Zhou, Y.; Fahlman, M.; Bo, Z.; Zhang, F. *Chem. Mater.* **2009**, *21*, 5327. (b) Zhao, X.; Piliego, C.; Kim, B.; Poulsen, D. A.; Ma, B.; Unruh, D. A.; Fréchet, J. M. J. *Chem. Mater.* **2010**, *22*, 2325. (c) Wong, W. Y.; Wang, X. Z.; He., Z.; Djurišic, A. B.; Yip, C. T.; Cheung, K. Y.; Wang, H.; Mak, C. S. K.; Chan, W. K. *Nat. Mater.* **2007**, *6*, 521. (d) Wang, Q.; Wong, W. Y. *Polym. Chem.* **2011**, *2*, 432.

(9) Steinberger, S.; Mishra, A.; Reinold, E.; Levichkov, J.; Uhrich, C.; Pfeiffer, M.; Bäuerle, P. *Chem. Commun.* **2011**, *47*, 1982.

(10) (a) Walker, B.; Tamayo, A. B.; Dang, X. D.; Zalar, P.; Seo, J. H.; Garcia, A.; Tantiwiwat, M.; Nguyen, T. Q. *Adv. Funct. Mater.* **2009**, *19*, 3063. (b) Loser, S.; Bruns, C. J.; Miyauchi, H.; Ortiz, R. P.; Facchetti, A.; Stupp, S. I.; Marks, T. J. *J. Am. Chem. Soc.* **2011**, *133*, 8142.

(11) Mei, J.; Graham, K. R.; Stalder, R.; Reynolds, J. R. *Org. Lett.* **2010**, *12*, 660.

(12) Leliège, A.; Blanchard, P.; Rousseau, T.; Roncali, J. *Org. Lett.* **2011**, *13*, 3098.

(13) (a) Rousseau, T.; Cravino, A.; Bura, T.; Ulrich, G.; Ziessel, R.; Roncali, J. *Chem. Commun.* **2009**, *13*, 1673. (b) Rousseau, T.; Cravino, A.; Bura, T.; Ulrich, G.; Ziessel, R.; Roncali, J. *J. Mater. Chem.* **2009**, *19*, 2298. (c) Rousseau, T.; Cravino, A.; Ripaud, E.; Leriche, P.; Rihn, S.; Nicola, A. D.; Ziessel, R.; Roncali, J. *Chem. Commun.* **2010**, *46*, 5082.

Table 1. Photochemical, Electrochemical, and Thermal Parameters for **BCNDTS** and **BDCDTS**

compd	λ_{abs} soln (nm)[a] (ε, M^{-1} cm^{-1})	λ_{abs} film (nm)[b]	ΔE^{opt} film (eV)[c]	$E_{ox}{}^{1}$ (V)[d]	$E_{red}{}^{1}$ (V)[e]	ΔE^{CV} (eV)[f]	HOMO (eV)[g]	LUMO (eV)[h]	T_d (°C)[i]
BCNDTS	553 (49984)	572	2.17	0.73	−1.36	2.09	−5.40	−3.23	378
BDCDTS	643 (78466)	659	1.88	0.71	−0.99	1.70	−5.80	−3.92	312

[a] Measured in CH_2Cl_2 solution (10^{-5} M). [b] Thin film on fused-silica substrate. [c] Estimated from λ_{abs} film. [d] Measured in CH_2Cl_2 solution with 0.1 M tetrabutylammonium hexafluorophosphate ($TBAPF_6$) as supporting electrolyte. [e] Measured in THF solution with 0.1 M tetrabutylammonium perchlorate (TBAP) as supporting electrolyte. All potentials were recorded versus ferrocene/ferrocenium (Fc/Fc^+) as an external reference. [f] Estimated from the difference between $E_{ox}{}^{1}$ and $E_{red}{}^{1}$. [g] Determined by ultraviolet photoelectron spectroscopy (UPS). [h] LUMO = HOMO + ΔE^{opt} film. [i] Temperature corresponding to 5% weight loss obtained from TGA analysis.

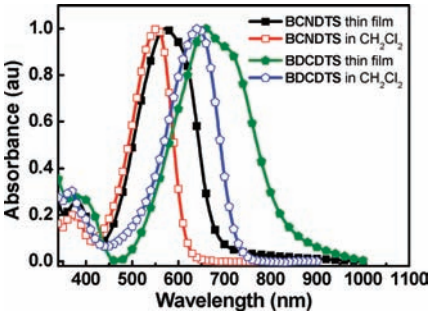

Figure 2. Normalized absorption spectra of **BCNDTS** and **BDCDTS** in CH_2Cl_2 and thin film.

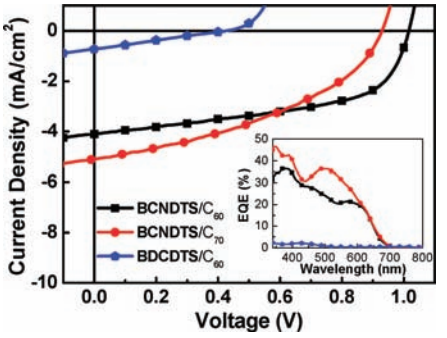

Figure 3. Current density−voltage characteristics (under AM 1.5G, 100 mW/cm^2 illumination) and EQE spectra (inset) of bilayer devices. The device structures are ITO/MoO_3 (5 nm) or PEDOT:PSS (30 nm)/**BCNDTS** or **BDCDTS** (8−10 nm)/C_{60} (35 nm) or C_{70} (15 nm)/BCP (10 nm)/Ag.

Normalized UV−vis absorption spectra of **BCNDTS** and **BDCDTS** are shown in Figure 2. In CH_2Cl_2 solution, **BCNDTS** and **BDCDTS** each show a featureless absorption band with a maximum at 553 and 643 nm, respectively. In comparison to the reported molecule composed of a DTS donor end-capped with BT acceptors (λ_{abs} at 503 nm),[17] these two tailor-made molecules exhibit evident bathochromic shifts in absorption, manifesting that enhanced solar spectral responses can be realized through our innovative molecular design. In contrast, the thin film absorption bands of **BCNDTS** and **BDCDTS** are broadened and red-shifted, which is probably stemmed from intermolecular $\pi-\pi$ stacking of the molecules in the solid states. Compared to the cyano end groups in **BCNDTS**, the stronger electron-withdrawing dicyanovinylene end groups endow **BDCDTS** with lower-lying molecular orbitals (LUMO), leading to a significantly reduced optical bandgap (Table 1).

The resulting absorption edge of the **BDCDTS** thin film even extends to 800 nm. Unfortunately, the combination of the stronger electron-withdrawing dicyanovinylene acceptors with electron-accepting BT moieties imparts **BDCDTS** thin films a higher electron affinity than fullerenes (as shown in the band diagram, Figure S2 in Supporting Information). Therefore, **BDCDTS** is hardly suitable to be paired with commonly used fullerene acceptors and the device data shown later also confirm this speculation.

Bilayer heterojunction (BLHJ) solar cells were first fabricated to evaluate the molecules for photovoltaic applications. The thicknesses of donor (**BCNDTS**, **BDCDTS**) and acceptor (C_{60}, C_{70}) layers have been tuned for accomplishing the best performance (Figures S3 and S4, Table S1 in Supporting Information). The current density−voltage (J-V) characteristics under AM 1.5G simulated solar illumination at an intensity of 100 mW/cm^2 and corresponding external quantum efficiency (EQE) spectra are shown in Figure 3. Note that, due to the inefficient electron transfer between **BDCDTS** and C_{60}, the **BDCDTS**/C_{60} cell

(14) (a) Ohshita, J.; Nodono, M.; Kai, H.; Watanabe, T.; Kunai, A.; Komaguchi, K.; Shiotani, M.; Adachi, A.; Okita, K.; Harima, Y.; Yamashita, K.; Ishikawa, M. *Organometallics* **1999**, *18*, 1453. (b) Hou, J.; Chen, H.-Y.; Zhang, S.; Li, G.; Yang, Y. *J. Am. Chem. Soc.* **2008**, *130*, 16144. (c) Lin, L.-Y.; Tsai, C.-H.; Wong, K.-T.; Huang, T.-W.; Hsieh, L.; Liu, S.-H.; Lin, H.-W.; Wu, C.-C.; Chou, S.-H.; Chen, S.-H.; Tsai, A.-I *J. Org. Chem.* **2010**, *75*, 4778. (d) Lin, H.-W.; Lin, L.-Y.; Chen Y.-H.; Chen, C.-W.; Lin, Y.-T.; Chiu, S.-W.; Wong, K.-T. *Chem. Commun.* **2011**, *47*, 7872.

(15) Chu, T.-Y.; Lu, J. P.; Beaupre, S.; Zhang, Y. G.; Pouliot, J.-R.; Wakim, S.; Zhou, J. Y.; Leclerc, M.; Li, Z.; Ding, J. F.; Tao, Y. *J. Am. Chem. Soc.* **2011**, *133*, 4250.

(16) Chen, H.-Y.; Hou, J.; Hayden, A. E.; Yang, H.; Houk, K. N.; Yang, Y. *Adv. Mater.* **2010**, *22*, 371.

(17) Welch, G. C.; Coffin, R.; Peet, J.; Bazan, G. C. *J. Am. Chem. Soc.* **2009**, *131*, 10802.

shows a low PCE of 0.07% (Table 2). In contrast, the device based on **BCNDTS**/C_{60} shows superior performance with a V_{OC} of 1.02 V, J_{SC} of 4.17 mA/cm^2, and fill factor (FF) of 0.54, thus improving the PCE to 2.3%. The **BCNDTS**/C_{70} BLHJ cell has also been fabricated and measured (Figures S5 and S6, Table S2, in Supporting Information). In comparison to the **BCNDTS**/C_{60} device, the **BCNDTS**/C_{70} cell exhibits a higher J_{SC} due to higher and broader extinction coefficients of C_{70} thin films. However, because of the lower electron mobilities of C_{70} thin films,[18] the device shows a lower FF of 0.41, which is only 76% of the **BCNDTS**/C_{60} device, resulting in a slightly lower efficiency of 1.9%. It is noteworthy that both **BCNDTS**/C_{60} and **BCNDTS**/C_{70} devices exhibit high V_{OC} values (up to 1.02 V), which can be ascribed to the deep-lying HOMO level (−5.4 eV, measured with ultraviolet photoelectron spectroscopy) of **BCNDTS** thin films.

Encouraged by the promising performance of BLHJ cells based on **BCNDTS**, planar mixed heterojunction (PMHJ) solar cells consisting of donor layer-donor:acceptor (1:1) mixed layer-acceptor layer as active layers were further investigated.[14d] (Figures S7 and S8, Table S3, in Supporting Information). Figure 4 shows the J-V characteristics and EQE spectra of PMHJ devices. Like the BLHJ solar cells, the higher J_{SC} value obtained in the **BCNDTS**:C_{70} device is attributed to higher extinction coefficients of C_{70} in the range of 380−470 nm, which can complement the absorption valley of **BCNDTS** thin films. Interestingly, the PMHJ **BCNDTS**:C_{60} and **BCNDTS**:C_{70} cells show similar FF values of about 0.34 (Table 2). This could be ascribed to the similar field-dependent carrier transport and recombination properties in **BCNDTS**:C_{60} and **BCNDTS**:C_{70} mixed layers. Consequently, the **BCNDTS**:C_{70} cells shows a superior PCE of 2.8%.

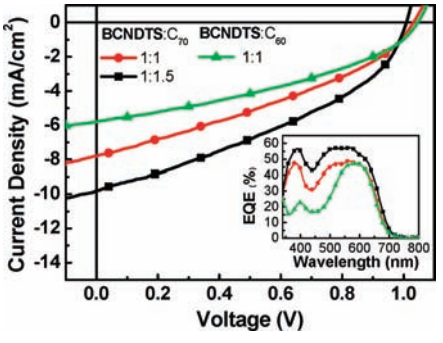

Figure 4. Current density−voltage characteristics (under AM 1.5G, 100 mW/cm^2 illumination) and EQE spectra (inset) of PMHJ devices. The device structures are ITO/MoO_3 (5 nm)/**BCNDTS** (7 nm)/**BCNDTS**:C_{60} or **BCNDTS**:C_{70} (40 nm)/C_{60} (20 nm) or C_{70} (7 nm)/BCP (10 nm)/Ag.

The performance of PMHJ devices are largely affected by BHJ properties of the donor−acceptor mixed layer, which could be manipulated either by post-treatments such as thermal/solvent annealing or changing the donor:acceptor ratio. Accordingly, various blend ratios (2:1, 1.5:1, 1:1, 1:1.5, and 1:2) of **BCNDTS** and C_{70} in PMHJ solar cells have been explored (Figures S9 and S10, Table S4, in Supporting Information). Increasing the concentration of C_{70} in mixed layer has a strong impact on the J_{SC}, while the V_{OC} is less dependent on the concentration of C_{70} as it is primarily dictated by the nature of the components. As shown in Figure 4, the best performance was obtained with the **BCNDTS**:C_{70} ratio at 1:1.5, giving a PCE of up to 3.7% with a V_{OC} of 1.01 V, J_{SC} of 9.79 mA/cm^2, and fill factor of 0.38 (Table 2). The results may indicate that this blend ratio yields a preferable phase separation and carrier transportation pathway in the mixed layer.

Table 2. Photovoltaic Parameters of Bilayer and Planar Mixed Heterojunction Solar Cells under AM 1.5 G Simulated Solar Illumination at an Intensity of 100 mW/cm^2

device type	J_{sc} (mA/cm^2)	V_{oc} (V)	FF	η (%)
BDCDTS/C_{60}[a]	0.73	0.43	0.24	0.07
BCNDTS/C_{60}[a]	4.17	1.02	0.54	2.3
BCNDTS/C_{70}[a]	5.11	0.93	0.41	1.9
BCNDTS:C_{60} (1:1)[b]	5.80	1.05	0.38	2.3
BCNDTS:C_{70} (1:1)[b]	7.81	1.03	0.34	2.8
BCNDTS:C_{70} (1:1.5)[b]	9.79	1.01	0.38	3.7

[a] Bilayer heterojunction configuration. [b] Planar mixed heterojunction configuration.

In summary, two new molecules (**BCNDTS** and **BDCDTS)** with an A-A-D-A-A molecular architecture have been synthesized. The side-by-side combination of two strong electron-withdrawing groups leads **BDCDTS** to exhibit a low optical bandgap. However, the overtuned LUMO level prohibits **BDCDTS** as an effective donor material in fullerene-based solar cells. In contrast, the thin film absorption spectrum and energy levels of **BCNDTS** show promising characteristics as efficient donor materials in SMOSCs. A PCE as high as 2.3% has been obtained with a simple bilayer structure. By adopting planar-mixed device structures and tuning the donor:acceptor ratio of the mixed layer, the PCE value has been further improved to 3.7% without extra thermal or solvent annealing processes. We believe that the present results can open up a new design concept to develop small molecule electron donors for highly efficient organic photovoltaics.

Acknowledgment. We would like to acknowledge National Science Council, Taiwan (NSC 98-2112-M-007-028-MY3, 98-2119-M-002-007-MY3), National Tsing Hua University, and National Taiwan University for financial support.

Supporting Information Available. Synthesis, characterization, copies of ^{1}H and ^{13}C NMR spectra, device fabrication, and optimization of solar cells. This material is available free of charge via the Internet at http://pubs.acs.org.

(18) Pfuetzner, S.; Meiss, J.; Petrich, A.; Riede, M.; Leo, K. *Appl. Phys. Lett.* **2009**, *94*, 223307.